ADVANCED ENGINEERING MATERIALS

DOI: 10.1002/adem.200700253

Iron Based Alloy with Hierarchical Structure and Superior Mechanical Performance**

By *Jian-Guo Wang*, *De-Qian Zhao*, *Ming-Xiang Pan* and *Wei-Hua Wang**

Natural materials such as bone, shell, and tooth with superior mechanical properties exhibit hierarchical structures from nanoscale to macroscale. This motivates us to improve the mechanical performance, in particular the plasticity and strength, of Fe-based metallic glass-forming alloys by transcribing natural biological designs into the alloys. Here, a Fe-based alloy was designed using a strategy of copious nucleation, positive mixing heat and high entropy of mixing, and prepared by simple casting method to obtain a hierarchical microstructure. The alloy is composed mainly of milli-scale lathy, micro-scale dendritic phases, nanoscale crystalline particles and a glassy matrix with short-range order of a length scale less than 1 nm. The alloy shows extraordinarily high strength and large ductility, high resistance to oxidation and corrosion, which are superior to most of the high-strength iron alloys. This makes the alloy a promising candidate for structural material, and the strategy is applicable to a broad range of metallic alloys and may serve as a design consideration for the development of structural metallic materials.

Structural materials, including poly-, ultrafine-, nano-crystalline metals and alloys and even amorphous alloys, require an optimized combination of strength and plasticity.[1–3] However, the two most important mechanical properties for structural materials usually sacrifice for each other.[3] Generally, coarse-grained metallic alloys exhibit high ductility but low yield and fracture strength, while amorphous alloys, especially bulk metallic glasses (BMGs), present super high strength but very limited plasticity (usually < 2 %).[4–7] Between the two extremes lie ultrafine- and nano-grained materials with fairish strength and plasticity.[8–11] Extensive efforts have been made for decades to combine the two utilizable mechanical properties by solid solution, grain refinement,[4] and heavy cold work[12] and so on. Despite extensive explorations and researches, the optimum mechanical properties combination remains a challenge.

Irons and steels, the most widely applicable structural materials, comprise well over 80 % by weight of the alloys in general industrial use.[4] Unfortunately, the strength of the irons and steels is severely limited due to the large crystalline grain, which is predicted by Hall-Petch equation.[4] Nanostructured Fe and Fe-based BMGs suffer shear localization once the onset of plastic deformation when compressed.[8,9,13] Although some of BMGs, such as Ti-, Zr-based BMGs, have been improved in plasticity by *ex situ*[14] or *in situ*[15,16] introduction of ductile crystalline phase in glassy matrix, little work is done to Fe-based BMGs[13] which often fracture in a very brittle manner (occasionally explosion-like[7]) when loaded. However, silica glass, a well-known inherently brittle material, is widely used as building material in biological world.[17,18] It is found that the hexactinellid sponge Euplectella sp. designs its skeleton at seven length scales from nanometer to centimeter: Nano-scaled silica spheres are settled in concentric rings which are glued together by organic matrix to form micro-scaled laminated spicules assembled into bundles and then these bundles produce a macroscopic structure.[19] On the other hand, an organic matrix hybrid composite with less than 5 % of volume fraction plays a critical role in the laminated architecture (polywoodlike) in that the organic layers can diverse and rechannel the crack and even prevent the spread of the crack, and the silica scaffold sustains exterior compression and tension.[18,19] As a result, Euplectella sp. possesses astonishing mechanical stability though silica glass is employed. So the silica glass delaminated and assisted by thin organic interlayers at hierarchical scales achieves ductility without any loss of strength. This stimulates us to apply this design to Fe-based BMG-forming alloys to overcome their brittleness and improve their strength and ductility simultaneously.

The recently developed Fe-based BMG-forming alloys, with a very stable supercooled liquid phase and high resistance against crystallization,[20,21] permit control of the nucleation and growth process in the supercooled liquid state and fabrication of various crystalline phases in different length scales through controllable solidification or annealing. This makes it possible to synthesize Fe-based alloys with hierarchical microstructures. In this work, a Fe-based BMG with superior glass forming ability was chosen as a starting point. By taking advantage of the strategies of copious nucleation, high

[*] *Prof. W. H. Wang, J. G. Wang, D. Q. Zhao, Dr. M. X. Pan*
Institute of Physics
Chinese Academy of Sciences
Beijing 100080, P. R. China
E-mail: whw@aphy.iphy.ac.cn

[**] *This work was supported by the Natural Science Foundation of China(Grant Nrs. 50621061 and 50731008) and the National Basic Research Program of China (MOST 973, grant No. 2007CB613904).*

entropy of mixing, and positive mixing heat, we obtain a Fe-based alloy with a structural hierarchy ranging from nanometer to millimeter through simple casting method. The ensuing hierarchical structure overcomes the brittleness of the Fe-based BMGs, and makes the alloy show outstanding mechanical properties. The mechanical benefits of each hierarchical level and mechanism for the superior mechanical properties of the alloy are discussed. The simple and convenient synthesis route on the basis of the appropriate choice of composition in BMG-forming alloy is a suggestive solution to the problem of brittleness in BMGs and might provide useful guidelines for the development of plastic alloys with high strength.

Herein, we present a new $Fe_{42}Co_{7.3}Ni_{16}Cr_{11.8}Cu_{6.3}C_{14.8}Y_{1.8}$ (at.%) alloy whose unique feature is the complex hierarchical microstructure as shown in Figure 1. The SEM image (Fig. 1(a)) of the sample mainly shows a crystalline lathy phase. The longest lath is 0.15 mm in length and most laths range from 0.06 to 0.10 mm, and 100 ~ 200 nm in thickness. The bright-field TEM image (Fig. 1(b)) of the sample also corroborates the existence of lathy phase. The HRTEM image (Inset I) clearly shows lattice fringes corresponding to crystalline nature of the lathy crystals, and the phase around the lathy crystals exhibits mazelike structure without any crystalline particle (Inset II), which indicates the glassy phase surrounding the crystalline phase. The Inset I of Figure 1(a) shows a dendritic phase with an average length of 11 μm dispersed homogeneously in the sample. The Inset II displays the XRD pattern indicating the dominant crystalline phase in the sample. Combining with the SEM electron microprobe composition analysis, it is inferred that the crystalline phase is the face centered cubic (fcc) Fe (Cr, C) solid solution. In addition, the nanocrystalline particles with an average size of ~ 3 nm are found embedded in the amorphous matrix (Fig. 1(c)). The microstructural investigation shows that the hierarchical structure continually ranges from amorphous (the short-range order or cluster length scale is less than 1 nm) to nano- to micro- and to milli-meter length scales. Figure 1(d) illustrates the microstructure of the sample. These results indicate that the approach is effective in forming complex composite with hierarchical structure in the BMG-forming alloys.

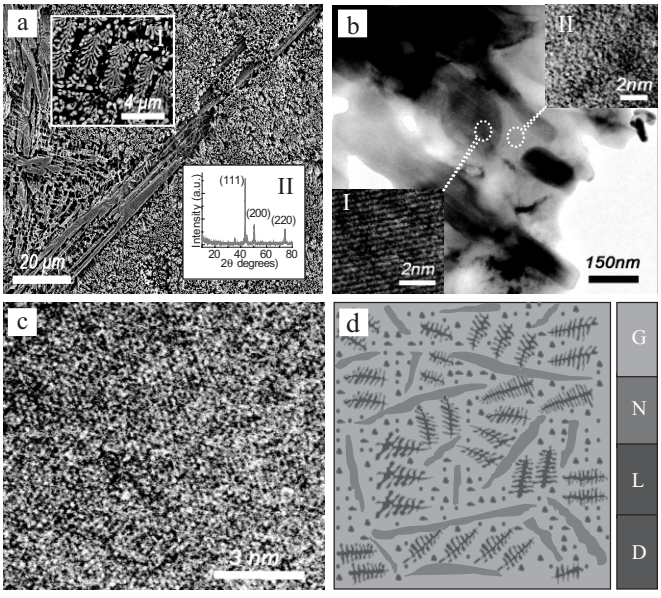

Fig. 1. Microstructures of the as-cast alloy: a) SEM image of in-situ formed lathy phase. (Inset I: dendritic phase; Inset II: XRD pattern of the alloy), b) Bright-field TEM image of crystalline phases. (Inset I: HRTEM image showing the crystalline nature of the lath, and Inset II: HRTEM image ascertaining the glassy state of the matrix), c) Bright-field HRTEM image of the nanostructured grains embedded in the amorphous matrix, d) Schematic illustration of hierarchical microstructure for the Fe-based alloy, G: glassy matrix; N: nanoparticles; D: dendritic phases; L: lathy phases.

The *in situ* formation of crystalline phases in different length scales is initiated through deviation from the best glass-forming composition of FeCoCrMoCBY[20,21] but using similar solidification conditions. SEM electron microprobe composition analysis shows that the nanoparticle phase is rich in Cu and Y while the dendritic phase is Cu rich and Y scarce and the lathy phase is Cu and Y scarce. The nanoparticles extensively dispersed in the sample result from the copious nucleation enhanced by addition of Cu which have positive mixing heat with Fe and other elements[22,23] and slow nuclei growth rate in the viscous alloy melt (Y element can stabilize the liquid phase and increase the viscosity of the melt[20]). The formation and growth of dendritic phase usually result from the negative temperature gradient in liquid phase and the trunks of most dendrites in a cylindrical specimen grow in the same direction from outer region (contact the wall of the copper mold) to inner region. However, the dendrites observed in this work are in a random orientation as illustrated in Figure 1(d). A similar situation happens to the lathy phase. The millimeter-sized laths, mainly containing Fe, Cr and C, separately form with a random orientation (Fig. 1(d)) unlike the laths in parallel arrays in traditional martensite and bainite which are usually processed by annealing.[4] The morphology and composition of the dendritic and lathy phases indicate that their formation is essentially controlled by the chemical composition instead of the temperature. For a conventional multicomponent alloy, a large number of imtermetallic phases or other complex phases would be expected to form. The resultant phases in our alloy are rather simple as indicated by XRD. This is due to the high entropy of mixing of the alloy containing seven elements, which significantly lowers the free energy, thus lowering the tendency to order and segregate and making random fcc Fe(Cr, C) solid solution in large size scale and amorphous phase more easily form and more stable than intermetallics or other ordered phases during solidification.[24]

Mechanical tests demonstrate the superior mechanical performance of the alloy with the hierarchical microstructure. Figure 2(a) shows the stress and train curve of the alloy in compressive test, and the inset is the true stress-true strain curve. The alloy yields at 1.70 GPa (σ_y) after 1.3 % elastic strain is measured and it undergoes 13.1 % engineering strain

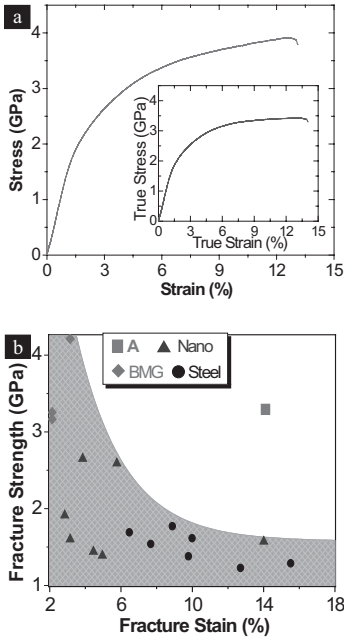

Fig. 2. Mechanical properties of the alloy, a) compressive stress-strain curve at ambient temperature. (Inset displaying the corresponding true stress-true strain curve), b) a comparison among some pure metals and alloys processed using different techniques and the Fe-based composites: The red square stands for the present alloy; the data for Steels from ref. [4]; Fe-based BMGs from ref. [5,6]; Nano-structured Fe and its alloys from ref. [8–11] The most structural materials have a strength-plasticity trade-off (the green region) while this Fe-based alloy has an optimum combination of strength and ductility (the red square).

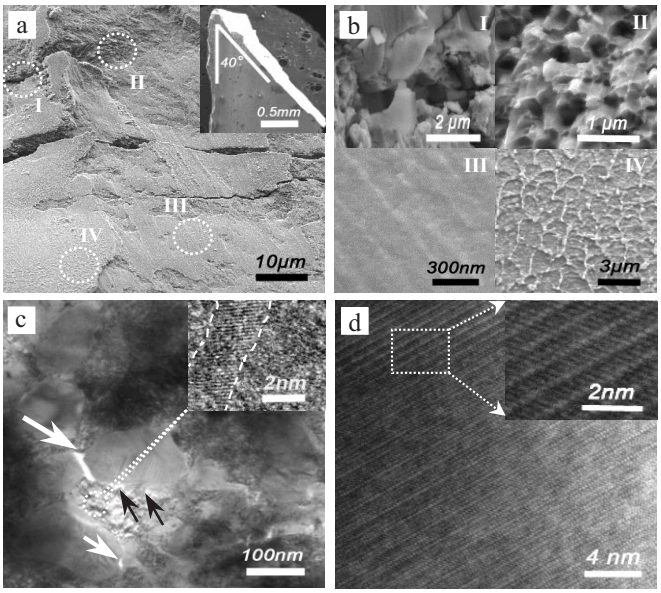

Fig. 3. Observations on fracture behaviors and deformation mechanisms of the failed alloy: a) SEM image of the fractured surface with different characteristic regions labeled by Roman numbers (Inset showing the side view of the fractured sample); b) SEM Images I-IV are the magnification of regions marked by I, II, III and IV in a); c), Bright-field TEM image of the deformed sample showing interaction between crystalline grains and microcracks: A large interganular crack (marked by large white arrow) is re-channeled to propagate along the boundary (marked by black arrows), and a smaller crack (marked by small white arrow) is blocked by nanoparticles (Inset HRTEM image of the grains and matrix in the fractured sample); d) HRTEM image exhibiting plenty of stacking faults in the deformed sample (Inset magnifying the rectangular area enclosed by dashed line).

and fractures with 3.79 GPa engineering stress (σ_f). The maximum stress reaches 3.90 GPa (σ_m) in excess of the fracture stress of most Fe-based BMGs.[5,7,13] In addition, evident work hardening can be seen in the true stress-true strain curve, which prevents instable flow and catastrophic fracture that usually happen in nano-materials and BMGs. Vickers hardness of the alloy is 5.27 GPa, much higher than that of stainless and super high strength steels,[5] which indicates that the alloy has a better rigidity. The ratio H/σ_y for this alloy is 3.1 in the range of that of metallic glasses (3 to 4.5) while for crystalline metals the ratio is ≤ 3.[25] Figure 2(b) presents a comparison among some pure metals and alloys processed using different techniques and the present Fe-based alloy. The most structural materials have a strength-plasticity trade-off, whereas the Fe-based alloy with hierarchical structure has an optimum combination of the high strength and the excellent ductility. Obviously, the multiscale microstructure obtained through appropriate choice of the composition and control of solidification conditions can remarkably improve the mechanical performance.

To understand the fracture behaviors of the alloy, the fractured samples were investigated in detail by SEM and TEM as shown in Figure 3. Various features (as labeled in Fig. 3(a)) are witnessed on the rough fracture surface. The compressive fracture angle is 40° (inset in Fig. 3(a)) which deviates from 45 ° for the maximum shear stress plane and approaches to that for most BMGs.[26] Transgranular fracture characteristics can be seen clearly in Figure 3(bI), which should be the rupture of the lath;[27] Figure 3(bII) shows a typical dimple structure, which is often observed on the fracture surface of nano-crystals fractured by torsion or tension,[28,29] indicates the ductility of the alloy induced by the nanoparticle phase in the glassy matrix. Some relatively smooth regions (marked by III in Fig. 3(a)) are detected, and no special feature can be observed even using large magnification (Fig. 3(bIII)). The vein pattern (Fig. 3(bIV)) similar to that on fracture surface of BMGs is observed, which could be attributed to the softening of the glassy phase in the alloy.[26] The plentiful morphologies on the fractograph also confirm the hierarchical structure of the alloy. Figure 3(c) shows microcracks developed during deformation. One can see that a large interganular crack is rechanneled to propagate along the boundary, and a smaller crack is blocked by the nanoparticles (see inset Fig. 3(c)). Figure 3(d) shows the massive stacking-faults in a crystalline grain and these stacking faults are not discovered in the as-cast sample. This indicates that the plastic deformation is mainly accommodated in the crystalline phase.

The glassy matrix accounts only for few voluminal percent of the alloy determined by differential scanning calorimetry (DSC). The glassy phase with a high elastic limit[30] is conducive to the high strength. Although the elastic strain limit (1.3 %) of the present alloy is lower than that of BMGs (~ 2 %)[5–7,16,30] it is much higher than that of conventional steels (0.2 ~ 0.6 %).[4] So the high yield stress of the alloy is

ADVANCED ENGINEERING MATERIALS

obtained owing to the extended elastic strain. A similar voluminal effect is found in biological materials such as mollusk shell and spicule of sponge that have a dominance (on the order of 95 % volume) of brittle ceramic component, but they have an astonishing toughness imparted by organic component of < 5 % volume.[18] Unlike other composites based on the glass-forming alloy,[14–16] no shear bands develop in the glassy matrix when the sample undergoes plastic strain. In contrast, the intergranular microcracks are rechannelled or blocked by the nano-crystalline phases in the glassy matrix. This makes the spread and linkup of microcracks quite difficult, thus prevents premature fracture. Ensuing strain has to be accommodated in the crystalline phases, resulting in strain hardening and therefore high fracture stress. As a result, more microcracks are created, especially near the fracture plane (images not shown), which in turn contributes to the toughness.[27] Eventually, a large main crack develops, and the sample is sheared off in terms of Mode II fracture.[27] Also, the dendrites and laths are inevitably sheared, especially in the fracture plane, preceded by the homogeneous deformation. The dendrites can improve the ductility markedly, because they have the capablity of deforming themselves by dislocation[16] and preventing shear localization with their branches;[15,16] the laths, which play a role of fibers in the alloy,[27] are embrittled by high carbon content like high-carbon steel. Nevertheless, the lathy phase is still more ductile than, and has high strength similar to, the glassy matrix when compressed or sheared.[4] These "fibers" contributes to toughness in two ways: One is to produce a closing force in the crack wake, and this force reduces the stress intensity in front of the crack; the other one is the work needed to deform the lath itself plastically and to pull the lath a distance out of the matrix.[27] When the stress reaches the maximum, the loaded sample usually begins to collapse. For most of BMGs, the collapse occurs suddenly because the maximum engineering stress which the BMGs can sustain is usually their fracture stress.[5–7] The present alloy can experience ~ 1 % strain with a strain rate of 2×10^{-4} s^{-1} when the stress decreases from σ_m to σ_f. The hierarchical structure prevents the alloy from failing catastrophically even if it is loaded to maximum engineering stress. Consequently, each level of the hierarchical microstructures individually contributes to the mechanical performance and they interplay in the deforming process so that both strength and ductility benefit from the cooperation.

The alloy also has excellent oxidation and corrosion resistance, which plays an essential role in structural materials exposed to normal or harsh environment in most cases.[1] The alloy remains brilliantly lustrous after spending eight months in air, and its corrosion rate in 1 *N* HCl solution is 0.16 mmy^{-1} much lower than that of some monolithic BMGs containing refractory element niobium.[31] The excellent resistance to oxidation and corrosion should be the result of carbon and chromium content.[32]

In summary, a Fe-based alloy, with a hierarchical structure and the optimum combination of high strength and large ductility and high resistance to corrosion and oxidation, is obtained by making use of copious nucleation and low growth rate, positive mixing heat, high mixing entropy of the alloy. The superior mechanical performance of the alloy is attributed to each level of the hierarchical microstructure and their interplay. The design strategy may provide guideline for future development of structural metallic materials with hierarchical microstructure and superior mechanical performance.

Experimental

We chosen the Fe-based alloys with minor composition deviation from the recently developed Fe-based BMG-forming alloys with a very stable supercooled liquid phase and high resistance against crystallization.[20,21] Then some crystalline phase would precipitate during the fabrication process. Because the melt of the alloy have high viscosity and high resistance against the crystalline phases growth, we can easily control the nucleation and growth process in the supercooled liquid state and fabricate various crystalline phases in different length scales through controllable solidification or annealing. The alloys have a nominal composition $Fe_{42}Co_{7.3}Ni_{16}Cr_{11.8}Cu_{6.3}C_{14.8}Y_{1.8}$ (at.%). Pure metals (99.95^wt.%) and high-purity carbon (99.99 %) were arc-melted together and the melting was repeated four times to ensure composition homogenerity, and then about 5 g master alloy was remelted and cast into 2.0 mm-diameter rod using water-cooled copper mould under Ti-gettered purified argon atmosphere. We control the solidification and nucleation, growth of crystalline phases through controlling the cooling rate by choice of different diameters of the samples.

The structure of the as-cast samples was analyzed by x-ray diffraction (XRD) using a MAC M03 XHF diffractometer with CuKa radiation. A Philips XL30 SEM with EDX and a TECNAIL-F20 TEM were used to analyze the microstructure of the samples. Differential scanning calorimetry (DSC) was conducted to determine the fraction of the glassy phases in the alloy under a purified argon atmosphere in a Perkin Elmer DSC-7 at a rate of 20 $Kmin^{-1}$.

Compressive properties were tested by using an Instron type testing machine with a strain rate of 2×10^{-4} s^{-1} at room temperature. The compression samples 2 mm in diameter have an aspect ratio of 2:1 were prepared according to ASTM (American society for testing and materials) standards. The failed samples were investigated by SEM and TEM. Vickers hardness was measured by a Vickers diamond pyramidal microhardness tester with a load of 300 g and a loading time of 10 s at room temperature using a Polyvar Met microhardness tester (Inspiration 2000 Ltd., UK), before which the samples were polished (1,200 grit, then 0.5 μm diamond).

The resistance of the alloy to corrosion was examined by weight loss after in 1 *N* HCl solution open to air at room temperature. The corrosion rate *R* was calculated by:

$$R = \frac{8.76 \times 10^7 \times (M_0 - M)}{STD} \quad (1)$$

where M_0 and M are the mass of the sample before and after corrosion, taken to be 0.1386 g and 0.1376 g, respectively; S is the total surface area, taken to be 0.5723 cm^2; T is the time for corrosion, taken to be 121.7 hrs; D is the density of the sample, taken to be 7,684.656 kg/m^3.

Received: September 29, 2007
Final version: November 16, 2007
Published online: January 28, 2008

[1] L. W. Fisher, *Selection of Eng. Mater. and Adhesives* Taylor & Francis, Boca Raton, **2005**.
[2] Y. H. Zhao, X. Z. Liao , S. Cheng, E. Ma, Y. T. Zhu, *Adv. Mater.* **2006**, *18*, 2280.
[3] R. Z. Valiev, *Nature* **2002**, *419*, 887.

[4] R. W. K. Honeycombe, *Steels Microstruct. and Properties* Edward Arnold, London, **1981**.
[5] A. Inoue, B. L. Shen, C. T. Chang, *Intermetall.* **2006**, *14*, 936.
[6] X. J. Gu, A. G. McDermott, S. J. Poon, G. J. Shiflet, *Appl. Phys. Lett.* **2006**, *88*, 211905.
[7] Q. J. Chen, J. Shen, D. L. Zhang, H. B. Fan, J. F. Sun, *J. Mater. Res.* **2007**, *22*, 358.
[8] D. Jia, K. T. Ramesh, E. Ma, *Scr. Mater.* **2000**, *42*, 73.
[9] Q. Wei, D. Jia, K. T. Ramesh, E. Ma, *Appl. Phys. Lett.* **2002**, *81*, 1240.
[10] I. Ucok, T. Ando, N. J. Grant, *Mater. Sci. Eng. A.* **1991**, *133*, 284.
[11] X. H. Chen, J. Lu, L. Lu, K. Lu, *Scr. Mater.* **2005**, *52*, 1069.
[12] Y. M. Wang, M. W. Chen, F. H. Zhou, E. Ma, *Nature* **2002**, *419*, 912.
[13] a) Y. H. Liu, G. Wang, R. J. Wang, D. Q. Zhao, M. X. Pan, W. H. Wang, *Sci.* **2007**, *315*, 1385. b) K. F. Yao, C. Q. Zhang, *Appl. Phys. Lett.* **2007**, *90*, 061901.
[14] C. Fan, H. Q. Li, L. J. Kecskes, K. X. Tao, H. Choo, P. K. Liaw, C. T. Liu, *Phys. Rev. Lett.* **2006**, *96*, 145506.
[15] C. C. Hays, C. P. Kim, W. L. Johnson, *Phys. Rev. Lett.* **2000**, *84*, 2901.
[16] G. He, J. Eckert, W. Loser, L. Schultz, *Nature Mater.* **2002**, *2*, 33.
[17] C. C. Perry, T. K. Tucker, *J. Biol. Inorg. Chem.* **2000**, *5*, 537.
[18] G. Mayer, *Sci.* **2005**, *310*, 1144.
[19] J. Aizenberg, J. C. Weaver, M. S. Thanawala, V. C. Sundar, D. E. Morse, P. Fratzl, *Science* **2005**, *309*, 275.
[20] V. Ponnambalm, S. J. Poon, G. J. Shiflet, *J. Mater. Res.* **2004**, *19*, 1320.
[21] J. Shen, Q. J. Chen, J. F. Sun, H. B. Fan, G. Wang, *Appl. Phys. Lett.* **2005**, *86*, 151907.
[22] A. L. Greer, *Nature* **1994**, *368*, 688.
[23] a) W. H. Wang, *Prog. Mater. Sci.* **2007**, *52*, 540. b) W. H. Wang, *J Appl. Phys.* **2006**, *99*, 093506. c) W. H. Wang, C. H. Shek, *Mater. Sci. Eng. R* **2004**, *44*, 45
[24] J. W. Yeh, S. K. Chen, S. J. Lin, J. Y. Gan, J. S. Chin, T. T. Shun, C. H. Tsau, S. Y. Chang, *Adv. Eng. Mater.* **2004**, *6*, 299.
[25] C. A. Schuh, T. C. Hufnagel, U. Ramamurty, *Acta Mater.* **2007**, *55*, 4067.
[26] Z. F. Zhang, G. He, J. Eckert, L. Schultz, *Phys. Rev. Lett.* **2003**, *91*, 045505.
[27] T. H. Courtney, *Mech. Behavior of Mater.* McGraw-Hill Company, Inc. **2000**.
[28] A. Hasnaoui, H. V. Swygenhoven, P. M. Derlet, *Science* **2003**, *300*, 1550.
[29] H. Q. Li, F. Ebrahimi, *Adv. Mater.* **2005**, *17*, 1969.
[30] A. R. Yavari, J. J. Lewandowski, J. Eckert, *MRS Bull.* **2007**, *32*, 635.
[31] C. L. Qin, W. Zhang, K. Asami, N. Ohtsu, A. Inoue, *Acta Mater.* **2005**, *53*, 3903.
[32] F. E. Luborsky, *Amorphous Metall. Alloys* Butterworths, USA, **1983**.

